Small Angle Neutron Scattering with Hydrogenated Amorphous $Cu_{50}Ti_{50}$ and Ni–Ti–Si Alloys

P. Lamparter

Max-Planck-Institut für Metallforschung, Institut für Werkstoffwissenschaft, D-70174 Stuttgart, FRG

B. Boucher

Service de Physique de l'Etat Condensé, Commissariat à l'Energie Atomique, CEN Saclay, F-91191 Gif-sur-Yvette, Cedex, France

Z. Naturforsch. **48a**, 1086–1092 (1993); received August 26, 1993

The metallic glasses $Cu_{50}Ti_{50}$, $Ni_{30}Ti_{60}Si_{10}$, $Ni_{32}Ti_{52}Si_{16}$, $Ni_{16}Ti_{68}Si_{16}$ and $Ti_{84}Si_{16}$ were produced by melt spinning. The alloys in the blank state as well as after loading with hydrogen or deuterium were investigated by small angle neutron (SANS) and X-ray (SAXS) scattering. The scattering of the different amorphous alloys exhibited common features. SANS follows a power-law with exponent of the scattering vector between -3 and -4. The melt-spun glasses contain extended structural inhomogeneities which are associated rather with the local composition than with the local density. SAXS measurements did not show effects above the background level.

Loading the alloys with hydrogen or deuterium causes strong effects in the SANS behaviour. From the results it is concluded that the amorphous alloys contain inner surfaces where the hydrogen atoms segregate.

1. Introduction

It has been found in recent years that many of the metallic amorphous alloys, the so-called metallic glasses, are not homogeneous, but exhibit fluctuations of their structural properties which may occur on length scales of some ten Å up to several thousand Å. In a diffraction experiment, using neutrons or X-rays, the associated fluctuations of the scattering length density gives rise to a small angle scattering effect.

The interpretation of small angle scattering effects as observed with metallic glasses is not trivial because quite different types of heterogeneities are possible, involving different local physical properties such as the density, the composition and the magnetization. Furthermore, these heterogeneities may occur in the bulk and/or at the outer surfaces of the material (for reviews see e.g. [1] and [2]).

Metallic glasses which contain an early-transition-metal as one of the constituents can incorporate large amounts of hydrogen. The distribution of the hydrogen atoms should be affected by the inhomogeneous structure of an amorphous alloy. Therefore it is expected that hydrogen can be employed as a probe for the nature of the heterogeneities. In the present work, melt-spun $Cu_{50}Ti_{50}$ and Ni–Ti–Si glasses were loaded with hydrogen and investigated by small angle neutron (SANS) and X-ray (SAXS) scattering. Isotopic substitution between hydrogen and deuterium was applied in order to make use of their opposite coherent scattering lengths as contrast variation method. Ti has a negative scattering length. Thus by choice of the Ni/Ti ratio, Ni–Ti–Si alloys with positive, zero and negative mean scattering length could be prepared.

Reprint requests to Dr. P. Lamparter, Max-Planck-Institut für Metallforschung, Institut für Werkstoffwissenschaft, Seestraße 92, D-70174 Stuttgart, FRG.

2. Experimental

2.1. Sample Preparation

The amorphous alloys $Cu_{50}Ti_{50}$, $Ni_{30}Ti_{60}Si_{10}$, $Ni_{32}Ti_{52}Si_{16}$, $Ni_{16}Ti_{68}Si_{16}$ and $Ti_{84}Si_{16}$ were produced by the melt spinning method as ribbons with a thickness between 20 µm and 30 µm and 1–2 mm wide. By X-ray wide angle diffraction the ribbons were proved to be fully amorphous. The hydrogen loading was done by electrolysis in a 1 M solution of H_2SO_4 (D_2SO_4) in H_2O (D_2O) with some AsO_3 as a hydrogen recombination poison. The electrolytic cell was made from some meters of the melt-spun ribbon wound on a cylindrical PVC frame as the cathode and a Pd wire in the center as the anode. The temperature,

0932-0784 / 93 / 1100-1086 $ 01.30/0. – Please order a reprint rather than making your own copy

between 40 °C and 60 °C, and the current density were chosen such that the H(D) loading was achieved within several hours. The H(D) content was analyzed using hot-extraction in combination with a gas chromatograph. It turned out to be non-uniform along the length of the ribbon with deviations up to 10 pct of the average value.

After loading with H(D), the surface of the ribbons was cleaned mechanically and ultrasonically. Some ribbons were also ground with sand paper. In all cases the electrolysis was accompanied by an etching of the specimens resulting in a reduction of their thickness.

2.2. SANS Experiments

The ribbons were mounted on a frame holding typically 40 layers, each consisting of 10 parallel aligned cut pieces. A cadmium mask, 10×10 mm^2, in front of the frame defined the amount of material exposed to the neutron beam, which was about 0.5 grams.

The small angle neutron scattering experiments were done on the instruments PAXY and PAXE at the Laboratoire Léon-Brillouin, CEA-CNRS, C.E. Saclay, France. Different combinations of the wavelength and the sample-detector distance were chosen to cover in overlapping runs the range $4 \times 10^{-3} \leq Q \leq 0.4$ Å^{-1} of the momentum transfer $Q = 4\pi \sin \Theta/\lambda$, where 2Θ = scattering angle and λ = wavelength. The scattering patterns on the 2-dimensional detector proved to be isotropic. That means that the so-called edge effect, which has been explained by refraction of the neutrons at the edges of the ribbons [3] and which causes an enhanced intensity in the direction perpendicular to the ribbons, was not significant in the present SANS measurements. Therefore the data could be integrated circularly. The conventional corrections for background and absorption were applied. The incoherent scattering signal from a vanadium standard in the range $Q > 0.1$ Å^{-1} was used as reference for the conversion of the measured data into absolute scattering units per volume. The coherent scattering lengths b used in the present study are listed in Table 1.

From the constant level of the incoherent scattering contribution from the hydrogen atoms at $Q > 0.15$ Å^{-1} the H content was evaluated. It showed a tendency to be higher than the corresponding value from hot-extraction by a factor up to 1.2. The values of the H content in Table 2 represent mean values of both methods.

Table 1. Coherent scattering lengths b [4].

	Cu	Ni	Ti	Si	H	D
b [10^{-12} cm]	0.772	1.03	−0.3438	0.4169	−0.3741	0.6674

Table 2. ϕ: blank alloys; H(D): loaded with hydrogen or deuterium. MS: melt-spun; E: etched during electrolysis; G: ground with sandpaper. $c_{H(D)}$: number of H(D) atoms per host atom. $\langle b \rangle$: mean coherent scattering length. $f_{H(D)}$: enhancement factor of SANS. $-s$: exponent of power-law scattering. *: SANS shows curvature in a log-log plot.

Alloy		Surface history	$c_{H(D)}$	$\langle b \rangle$ [10^{-12} cm]	$f_{H(D)}$	$-s$
$Cu_{50}Ti_{50}$	ϕ	MS		0.598		−3.1
	H	E, G	0.15		3.7	−2.9
	D	E, G	0.15		7.4	*
$Ni_{30}Ti_{60}Si_{10}$	ϕ	MS		0.144		−2.8
	H	E	0.16		1.8	−2.8
	D	E, G	0.16		8.2	−3.2
$Ni_{32}Ti_{52}Si_{16}$	ϕ	MS		0.217		−3.3
	H	E	0.20		1.2	−3.2
	D	E	0.20		6.2	*
$Ni_{16}Ti_{68}Si_{16}$	ϕ	MS		0.0		−3.6
	H	E	0.75		0.5	−3.7
	D	E	0.75		1.8	−3.2
$Ti_{84}Si_{16}$	ϕ	MS		−0.222		−3.1
	H	E	0.62		1.5	−3.3
	D	E, G	0.62		4.4	*

2.3. SAXS Experiments

Small angle X-ray scattering measurements were performed in the range $Q > 10^{-2}$ Å^{-1} using a Kratky camera. Neither with the melt-spun samples, nor after loading with hydrogen a detectable increase of the intensity versus small Q-values was observed.

3. Results

Figure 1 shows the SANS curves as log $I(Q)$ versus log Q plots. In this representation a constant was subtracted from $I(Q)$ of the hydrogenated or deuterated samples chosen such that the level $B = I(Q > 0.1)$ became the same as for the corresponding blank sample. The following features were observed:

i) The melt-spun samples exhibit a SANS effect in the range $Q < 0.1$ Å^{-1}. The run of log $I(Q)$ versus log Q is linear in the region of small Q with slope $-s$, which corresponds to a power-law scattering

$$I(Q) = AQ^{-s} + B\,. \tag{1}$$

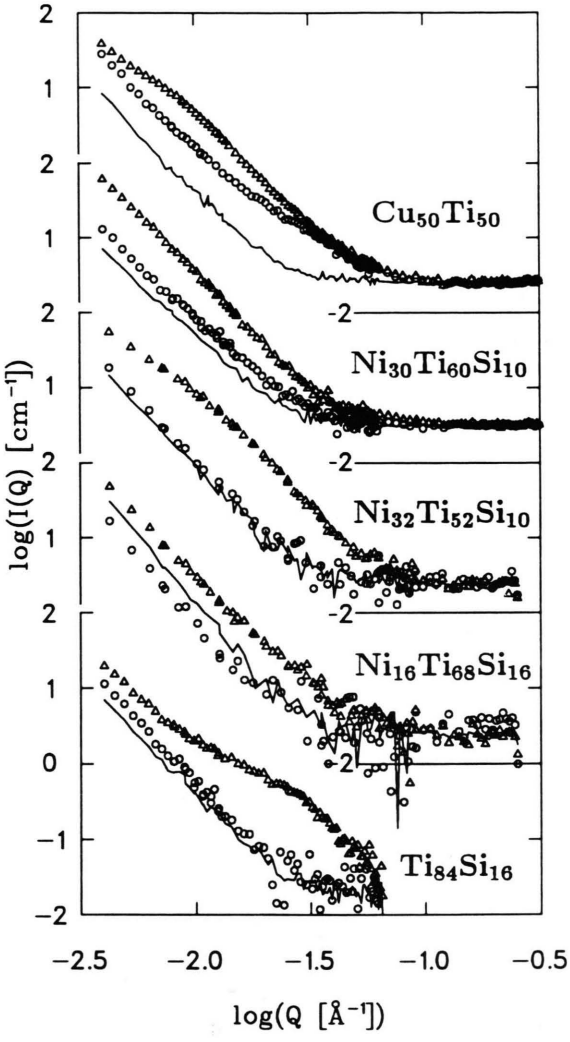

Fig. 1. SANS with amorphous $Cu_{50}Ti_{50}$ and Ni–Ti–Si alloys: log-log plot of the intensity $I(Q)$ versus Q. (——) blank samples after melt spinning, (○) loaded with hydrogen, (△) loaded with deuterium.

B represents the constant contributions from other effects, such as the incoherent scattering, the isothermal compressibility, etc. The values of the exponent $-s$ are listed in Table 2. There is no significant dependence of the SANS effect on the specific alloy system. In particular, it does not depend on the value of the mean scattering length $\langle b \rangle$ of the alloy (see Table 2).

(ii) Loading with hydrogen or deuterium affects strongly the intensity of the SANS signal. In most of the alloys hydrogen causes an increase of the SANS, but in $Ni_{16}Ti_{68}Si_{16}$ it leads to a decrease. Deuterium leads in all cases to an increase. The general behaviour

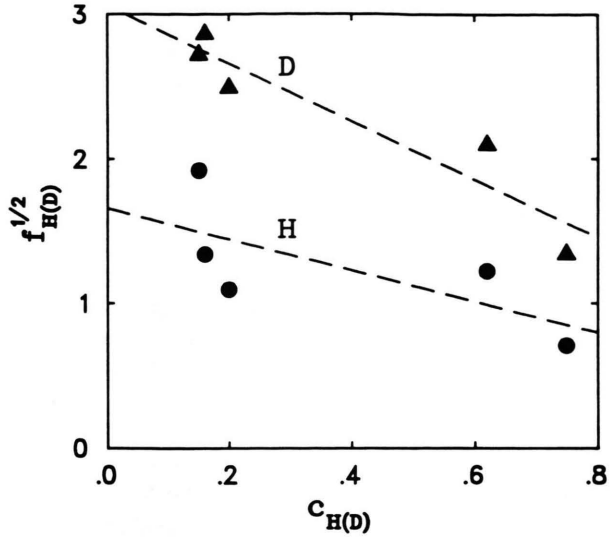

Fig. 2. Square root of the enhancement factor $f_{H(D)}$ of the SANS after H(D) loading versus the H(D) content $c_{H(D)}$. (●) hydrogen, (▲) deuterium, (– – –) lines from least squares fit.

of the scattering is less affected upon H(D) loading. In particular, there is no significant change of the power $-s$ (Table 2). The SANS curves of some deuterated alloys exhibit a curvature in Fig. 1, indicating an additional scattering effect which is superimposed on the power-law scattering.

The effect of H(D) loading on the overall SANS can be described by a multiplication factor $f_{H(D)}$:

$$\int I_{H(D)}(Q)\,dQ = f_{H(D)} \int I_{\phi}(Q)\,dQ\,. \qquad (2)$$

The values of $f_{H(D)}$ are listed in Table 2. For the values averaged over the five alloys we find the ratio

$$\langle f_D \rangle : \langle f_H \rangle = 3.5\,.$$

This value agrees well with the ratio of the squares of the scattering lengths of D and H

$$b_D^2 : b_H^2 = 3.2\,.$$

Figure 2 shows the dependence of the square root of $f_{H(D)}$ on the H(D) content $c_{H(D)}$. The observed decrease of the effect on the SANS upon H(D) loading with increasing H(D) content is a quite surprising result.

4. Discussion

For theoretical descriptions of small angle scattering phenomena we refer to [5] and [6]. Generally, small

angle scattering is caused by a non-uniform distribution of the scattering length density $\eta(R)$:

$$\eta(R) = \varrho(R)\, b(R)\,, \tag{3}$$

where $\varrho(R)$ = local atomic number-density at point R, $b(R)$ = local mean scattering length per atom.

Fluctuations of $\eta(R)$ can be either due to the density $\varrho(R)$ or to the composition $c(R)$. Note that fluctuations of $c(R)$ yield those of $b(R)$ if the constituents have different scattering lengths.

With various metallic glasses a SANS effect has been found in the range $Q > 0.1$ Å^{-1}, exhibiting a Guinier behaviour or even a diffraction peak. This has been attributed frequently to microsegregation into two different amorphous phases occurring on length scales of some ten Å [1, 2]. The curves in Fig. 1 do not show any SANS effect in the range $Q > 0.1$ Å^{-1}, and we state that there is no microsegregation in the metallic glasses studied in the present work. The fluctuations giving rise to SANS at $Q < 10^{-1}$ Å in the present study occur on a more extended scale of lengths.

In the following we discuss the present SANS results in the light of different types of extended structural inhomogeneities as possible sources.

4.1. Scattering from the Outer Surfaces

In recent years it has been shown that irregularities on the outer surfaces of amorphous ribbons or foils must be considered carefully as possible source of SANS [7, 8]. With the immersion technique [7] such effects can be suppressed. The specimen is surrounded by an immersion liquid chosen such that its mean scattering length density η is the same as that of the specimen and thus no contrast exists between the sample and its environment. An alternative possibility is to adjust the scattering length density of the sample. For the $Ni_{16}Ti_{68}Si_{16}$ glass η is zero (Table 2), i.e., the same as that of the surrounding air. Therefore there should be no, or a negligible surface contribution to the observed SANS. However, just with this alloy the SANS signal is the strongest of the blank alloys (Fig 1), and we conclude that it originates from the bulk.

SANS from an irregular sample surface is expected to be sensitive to the specific treatment of the surface. The samples in the present study were treated in quite different ways (see Table 2). Nevertheless, we found no indication that a specific treatment, such as grinding with sandpaper, led to a SANS signal which differed from that of the other specimens.

4.2. Density and Concentration Fluctuations

The scattering from fluctuations of the local atomic number-density $\varrho(R)$ scales with $\langle b\rangle^2$ of the alloy, whereas the scattering from fluctuations of the local concentration $c(R)$ depends on the differences of the scattering lengths of the involved constituents. The $Ni_{16}Ti_{68}Si_{16}$ glass without hydrogen displays the largest SANS signal of the blank alloys in spite of its mean scattering length $\langle b\rangle = 0$. Therefore it cannot be caused by fluctuations of the local density but must be due to compositional fluctuations. Of course, the latter in turn give rise also to density fluctuations depending on the different molar volumes of the constituents.

We note that in the case of density fluctuations as the only type of heterogeneities in the melt-spun glasses without H(D) it is expected that X-rays yield the same small angle scattering results as neutrons. However, no SAXS effect comparable to the results from SANS was found with the alloys investigated in the present work. Due to the negative neutron scattering length of Ti the differences of the b-values of the constituents are quite large, and SANS is therefore sensitive to concentration fluctuations. For X-rays the differences in scattering lengths are much smaller and presumably too small to result in any observable contrast.

4.3. Phase Separation

The SANS curves in Fig. 1 show a continuous rise towards the smallest Q-value, $Q = 4\times10^{-3}$ Å^{-1}, with a power-law according to (1). A Guinier regime, if existing at all, must be located below this Q-value. This implies that regions which differ in their composition from the matrix should have dimensions in the order of some 1000 Å or more.

In the following we discuss the influence of H(D) incorporation as would be expected for the presence of large phase separated regions. In order to simplify the qualitative considerations we assume that the separation involves a non-uniform distribution of the Ti atoms, whereas the ratio c_{Ni}/c_{Si} is uniform. Furthermore, we neglect the presence of density fluctuations. Then from (3) the contrast between the two phases for

the blank (ϕ) alloys follows as

$$\Delta\eta_\phi = \varrho_\phi \, \Delta c_{Ti} [b_{Ti} - b_c] , \qquad (4)$$

where Δc_{Ti} = compositional difference between the two phases, ϱ_ϕ = number density of the alloy, and b_c = average scattering length of the other component, Cu or (Ni, Si). We choose the notation such that $\Delta c_{Ti} > 0$ and accordingly $\Delta\eta_\phi < 0$. Wide angle scattering with Ti-containing hydrogenated metallic glasses proved that the hydrogen atoms prefer Ti nearest neighbours and that they do not affect substantially the number-density of the host matrix [9, 10]. Thus the influence of H (D) loading can be described simply by adding the scattering length of H (D) to that of the Ti atoms, and the contrast between the two phases can be written as

$$\Delta\eta_{H(D)} = \varrho_\phi \, \Delta c_{Ti} [(b_{Ti} + n_{H(D)} \, b_{H(D)}) - b_c] . \qquad (5)$$

$n_{H(D)} = c_{H(D)}/c_{Ti}$ is the number of H (D) atoms per Ti atom, and $c_{H(D)}$ is the number of H (D) atoms per atom of the host matrix. Equation (5) together with the b-values in Table 1 shows that below a certain H (D) content $c^r_{H(D)}$ the influence of H and D is expected to be opposite: Hydrogen always increases the contrast ($\Delta\eta_H$ becoming more negative), whereas addition of deuterium below c^r_D causes a decrease ($\Delta\eta_D$ becoming less negative). At a certain concentration $c_D = c^r_D$, referred to as point of reversal in the following, the contrast $\Delta\eta_D$ becomes zero and the SANS should vanish. Further addition of deuterium then should lead to an increase of the contrast ($\Delta\eta_D$ becoming positive). This means that above $c^r_{H(D)}$ the influence of H and D on the SANS should go into the same direction, i.e. an increase of the square of the contrast $(\Delta\eta)^2$ which rules the small angle scattering intensity $I(Q)$. The values c^r_D for the point of reversal, calculated from the scattering lengths, are in the order of one D atom per host atom.

The SANS results of the present work are in contradiction with the conclusions deduced from (5). The addition of deuterium, either at low or high c_D, caused an increase of the SANS instead of a decrease. Furthermore, the enhancement of the SANS signal by hydrogen was found to be smaller at higher c_H (Fig. 2), whereas from (5) it is expected that the enhancement scales with c_H. In conclusion of this section we state that a phase separation model is not appropriate to explain the experimental results using SANS in combination with hydrogen or deuterium as probe.

4.4. Inner Surfaces

Besides phase separation several models have been proposed in the past to account for a power-law scattering according to (1) with exponents between -3 and -4.

In [11] and [1] a model has been described where the amorphous system consists of large domains in the order of some 1000 Å. Introducing appropriate profiles of the scattering length density near the boundaries of the domains, experimental scattering laws could be reproduced. In [2] inner self-similar surfaces with fractal properties were proposed. Their fractal dimension D_s follows from the exponent $-s$ as $2 \leq D_s = 6 - s \leq 3$ [12]. In [13] a scattering law with exponent $-s = -3$ has been discussed in the frame of an internal stress field with the same spatial variation as caused by edge dislocations in crystalline materials [14]. Although we know in the meanwhile that compositional fluctuations rather than those of the density are the source of SANS in metallic glasses, it is important to bear in mind also one-dimensional defects as possible source.

In order to make further progress it will be important in future SANS experiments to extend the covered Q-range to smaller Q-values, say down to $Q = 10^{-5}$ Å^{-1}, by using ultra-SANS techniques. Note that in the present study the Q-range where a SANS effect is observed extends roughly over one decade. It will be interesting to investigate if there occurs a Guinier regime at very small Q, possibly yielding information about characteristic lengths of extended inhomogeneities.

In the following a qualitative interpretation of the present SANS results will be given on the base of inner surfaces as illustrated in Figure 3. The considerations are restricted to those features which the investigated amorphous alloys have in common, such as the power-law scattering. Individual features, like the curvature of the SANS of some deuterated samples as mentioned above, will not be considered.

The experimental facts that the influence of H an D loading on the SANS goes into the same direction and that it scales with the square of the scattering lengths of H and D ($\langle f_D \rangle : \langle f_H \rangle = 3.5$) implies that the concentration $c^r_{H(D)}$ of a point of reversal, if existent, must be substantially smaller than the H (D) contents of the samples in the present work.

The low level of H (D), sufficient to cause the essential changes in the SANS, indicates that the heterogeneities in spite of their large extension involve only

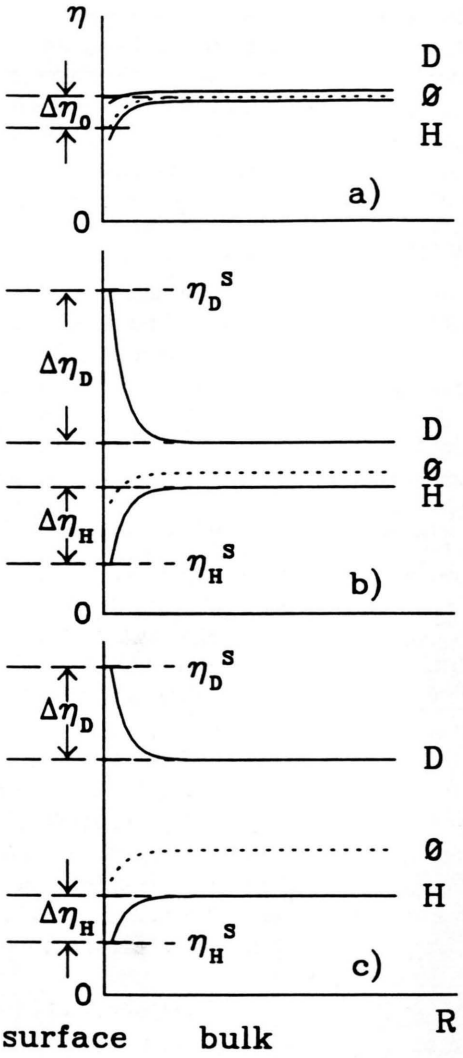

Fig. 3. Sketch of the scattering length density η at an inner surface and in the bulk. ϕ: blank sample; H: loaded with hydrogen; D: loaded with deuterium. From a) to c) the H(D) content is increasing. η^s_H, $\eta^s{}_D$ = saturation values of the scattering length density at the surface.

a small fraction of the volume of the system. Therefore defects with dimension smaller than 3 are suggested, such as inner surfaces or even line shaped defects. In the vicinity of the defects the local composition and presumably also the local density deviate from the values in the bulk, which causes a corresponding deviation of the scattering length density $\eta(R)$ as sketched in Figure 3. We assume that in the blank alloy the scattering length density at an inner surface is lower than in the bulk by $\Delta\eta_\phi$.

Hydrogen or deuterium atoms incorporated in the amorphous system segregate at the inner surfaces. At low concentration $c_{H(D)}$ the positive scattering length of the deuterium causes a decrease of the contrast, $\Delta\eta_D < \Delta\eta_\phi$, and hydrogen causes an increase, $\Delta\eta_H > \Delta\eta_\phi$, as sketched in Figure 3a. At a certain concentration c^r_D the point of reversal is reached where $\Delta\eta_D$ becomes zero (note that already at a low level of c_D, the concentration of segregated D atoms in the inner surfaces may be high). The situation in Fig. 3a and also the point of reversal would occur in Fig. 2 at concentrations $c_{H(D)}$ below the experimental points. Beyond $c^r_{H(D)}$ the influence of H and D goes into the same direction, causing an increase of $\Delta\eta_{H(D)}$ as shown in Figure 3b. The behaviour of $\Delta\eta_{H(D)}$ with further increase of $c_{H(D)}$ can be understood on the basis that the amount of H(D) at the inner surface saturates at a certain level corresponding to the scattering length density $\eta^s_{H(D)}$ at the surface. Due to the finite number of available sites the amount of hydrogen atoms in the surface reaches saturation already at low H(D) doping grades (Figure 3b). Further addition of H(D) enhances only the concentration in the bulk (Fig. 3c) and thus leads to the effect that at high H(D) concentration the contrast $\Delta\eta_{H(D)}$, and thus the SANS, is lowered.

In the present work the level of saturation is apparently reached already with the samples at low H(D) content $c_{H(D)} < 0.2$ because the samples with higher H(D) content show a decrease of the SANS effect (Figure 2). On the basis of the present explanation a maximum of $f_{H(D)}$ would be expected somewhere between $c_{H(D)} = 0$ and $c_{H(D)} = 0.15$.

The dashed lines in Fig. 2 were obtained by least squares fit. It is interesting to note that they extrapolate to a hypothetical point of zero contrast $f_{H(D)} = 0$ at the same concentration $c_H = c_D = 1.53$. This may be taken as an estimation of the number of hydrogen atoms per host atom in the saturated inner surfaces if we expect zero contrast for a situation where the H(D) content in the bulk is the same as in the surfaces. However, this interpretation is rather speculative: First, a system with uniform H(D) distribution should still exhibit the contrast as observed with the blank system before H(D) loading. Secondly, at very high H(D) contents the change of the structure of the host matrix itself may become considerable and the view that the H(D) atoms simply fill up the free sites in a given structure may no longer hold.

Concluding this section we note that, concerning an H(D) content at maximum contrast as well the existence of a point of reversal $c^r_{H(D)}$, it will be necessary to investigate amorphous alloys at lower H(D) content, preferably in an experimental set up where hydrogen loading from the gaseous phase and SANS measurements can be performed in-situ.

5. Conclusion

Amorphous melt-spun $Cu_{50}Ti_{50}$ and Ni–Ti–Si alloys contain extended fluctuations of the local composition which give rise to a small angle neutron scattering effect. The influence of hydrogen absorption on the scattering behaviour suggests inner surfaces as sites for the segregation of the hydrogen atoms. The amount of hydrogen in the surfaces reaches a saturation value already at low overall hydrogen content.

Acknowledgements

Thanks are due to A. Brulet, LLB Saclay, for help during the SANS experiments. We would also like to thank Laboratoire Léon Brillouin for allocation of beam time.

[1] B. Boucher and P. Chieux, J. Phys.: Condens. Matter **3,** 2207 (1991).
[2] P. Lamparter and S. Steeb, J. Non-Cryst. Sol. **106,** 137 (1988).
[3] M. Maret, P. Chieux, and H. Hicter, Z. Phys. Chem., N.F. **157,** 109 (1988).
[4] L. Koester and E. Seyman, Atomic Data and Nuclear Data Tables **49,** 65 (1991).
[5] A. Guinier and G. Fournet, Small Angle Scattering of X-Rays, John Wiley, New York 1955.
[6] O. Glatter and O. Kratky, Small Angle X-Ray Scattering, Academic Press, New York 1982.
[7] B. Rodmacq, Ph. Mangin, and A. Chamberod, Phys. Rev. **B 30,** 6188 (1984).
[8] H. Träuble, P. Lamparter, and S. Steeb, J. Phys. I France **2,** 1029 (1992).
[9] B. Rodmacq, Ph. Mangin, and A. Chamberod, J. Phys. F: Met. Phys. **15,** 2259 (1985).
[10] P. Lamparter and S. Steeb, Physica **B 180 & 181,** 782 (1992).
[11] B. Boucher, P. Chieux, P. Convert, and M. Tournarie, J. Phys. F: Met. Phys. **13,** 1339 (1983).
[12] J. E. Martin and A. J. Hurd, J. Appl. Cryst. **20,** 61 (1987).
[13] E. Nold, S. Steeb, and P. Lamparter, Z. Naturforsch. **35a,** 610 (1980).
[14] H. H. Atkinson and P. B. Hirsch, Phil. Mag. **3,** 213 (1958).